Inorg. Chem. **1984**, *23*, 3645-3649 **3645**

Contribution from the Institute of Inorganic Chemistry,
University of Basel, CH-4056 Basel, Switzerland

Investigation of Solution Kinetics of Transition-Metal Complexes by EPR Spectroscopy

HARALD GAMPP

Received December 22, 1983

The kinetics of the hydrolysis of the complex formed between copper(II) and 4,7,10-triazatridecanedinitrile (NIT) in 0.5 M aqueous NaOH have been studied by EPR spectroscopy. Representation of the digitized spectra in their eigenvector basis significantly reduces the amount of data to be handled in the subsequent numerical treatment and also shows that three different complexes are present in solution. The reaction can be described by two first-order consecutive steps: **1** → **2** → **3**. Rate constants ($k_{12} = 3.55 \times 10^{-4}$ s^{-1}, $k_{23} = 8.5 \times 10^{-5}$ s^{-1}) and solution EPR spectra of the complexes ($g_{av} = 2.125, 2.111, 2.103$) were calculated with use of a program based on Marquardt's modification of the Newton-Gauss nonlinear least-squares method. No information with respect to the EPR spectra of the species is needed, which makes the mathematical technique especially useful if several complexes are formed simultaneously and if their spectra are unknown and/or strongly overlapping. Spectral evidence suggests a mechanism, where in a first step one of the nitrile groups is converted into an amide, which is protected from further hydrolysis by equatorially coordinating to the copper. In a second, slower reaction the remaining nitrile is hydrolyzed. The results of this study show that EPR spectroscopy can be an alternative method for the investigation of solution kinetics of transition-metal complexes.

Introduction

EPR spectroscopy is a valuable tool for the study of kinetics and mechanisms of reactions of radicals in solution.[1] Generating the radicals by UV photolysis of samples within the cavity of an EPR spectrometer[2] allows one to follow the kinetics of short-lived species. Highly reactive intermediates can be identified by the use of spin traps[3] like nitroso compounds or *N*-oxides.[4-6] A wide range of reaction rates can be covered by using experimental techniques like continuous-flow,[7,8] stopped-flow,[9] rotating sector,[10,11] and modulation spectroscopy[12,13] or laser flash photolysis.[13-15]

If the observed EPR signal is due to a single species, its concentration can be obtained by doubly integrating the first-derivative spectrum obtained at a certain time.[7b] Because most of the studies are made on organic radicals giving rise to rather narrow lines, in cases with more than one species and overlapping spectra, the respective concentrations can be obtained by double integration of appropriate lines.[16]

In contrast to the widespread use of EPR in kinetic studies of organic radicals, the method is only occasionally applied for the investigation of kinetics of transition-metal complexes.[17] EPR line broadening has been used for studying the rapid ligand exchange at axial positions of square-planar vanadyl[18,19] and cupric[20,21] complexes. Paramagnetic intermediates formed during reactions of organometallic compounds could be identified by using spin trapping.[22,23] Continuous-flow methods were used to study the oxidation of V(IV)[24] and Ti(III)[8,25] by H_2O_2. In those cases, the observed spectra consisted of rather sharp lines and the radical concentrations could be obtained by simple graphical integration.

Very often, however, transition-metal complexes give rise to broad solution spectra,[26,27] and overlapping in multicomponent systems prevents the straightforward analysis, which is possible in the case of organic radicals.[16] The situation is thus closely similar to the one encountered in spectrophotometry, where numerical problems due to overlapping restricted the use of the method to relatively simple systems.[28,29] For data of high quality,[29] these problems have been successfully overcome: (i) Representation of the measured spectra in their eigenvector space significantly reduces the amount of data to be handled in the numerical treatment, allows one to do the complete calculation on a desk computer, and gives the number of absorbing species present.[30] (ii) Stability constants and spectra are calculated by using a procedure that does not need any information with regard to the complex spectra. This makes the method particularly useful if several complexes are formed simultaneously and if their spectra are unknown and/or strongly overlapping.[30,31]

It could be shown recently[32] that the same algorithm allows one to determine stability constants and spectra from EPR data. A similar approach will be presented here for the investigation of solution kinetics of transition-metal complexes. As an example, the hydrolysis of the cupric complex of 4,7,10-triazatridecanedinitrile (NIT) in 0.5 M aqueous NaOH was studied by EPR spectroscopy.

Experimental Section

Materials. NaOH (Merck, titrisol), KCl, and $CuSO_4 \cdot 5H_2O$ (Merck, p.A. grade) were used without further purification; water was doubly distilled.

4,7,10-Triazatridecanedinitrile trihydrochloride had been synthesized by condensation of dien and acrylonitrile and was obtained from Dr. M. Maeder.[33a] Hydrolysis of NIT in concentrated HCl

---

(1) Griller, D.; Ingold, K. U. *Acc. Chem. Res.* **1980**, *13*, 193.
(2) Griller, D. *Magn. Reson. Rev.* **1979**, *5*, 1.
(3) Janzen, E. G. *Acc. Chem. Res.* **1971**, *4*, 31.
(4) Ledwith, A.; Russell, P. J. *J. Chem. Soc., Perkin Trans 2* **1974**, 582.
(5) Chandra, H.; Davidson, I. M. T.; Symons, M. C. R. *J. Chem. Soc., Perkin Trans. 2* **1982**, 1353.
(6) Rosenthal, I.; Mossoba, M. M.; Riesz, P. *J. Magn. Reson.* **1982**, *47*, 200.
(7) (a) Ohno, K. *J. Magn. Reson.* **1982**, *49*, 56. (b) Adamic, K.; Bowman, D. F.; Gillan, T.; Ingold, K. U. *J. Am. Chem. Soc.* **1971**, *93*, 902.
(8) (a) James, R. E.; Sicilio, F. *J. Phys. Chem.* **1970**, *74*, 1166. (b) Czapski, G.; Samuni, A.; Meiser, D. *Ibid.* **1971**, *75*, 3271.
(9) Klimes, N.; Lassmann, G.; Ebert, B. *J. Magn. Reson.* **1980**, *37*, 53.
(10) Weiner, S.; Hammond, G. S. *J. Am. Chem. Soc.* **1968**, *90*, 1659; *Ibid.* **1969**, *91*, 986.
(11) Ingold, K. U. "Free Radicals"; Kochi, J. K., Ed.; Wiley: New York, 1973; Vol. 1, Chapter 2.
(12) Paul, H. *Int. J. Chem. Kinet.* **1979**, *11*, 495.
(13) Paul, H.; Small, R. D., Jr.; Scaiano, J. C. *J. Am. Chem. Soc.* **1978**, *100*, 4520.
(14) Small, R. D., Jr.; Scaiano, J. C. *J. Am. Chem. Soc.* **1978**, *100*, 296.
(15) Wong, S. K. *J. Am. Chem. Soc.* **1979**, *101*, 1235.
(16) Maillard, B.; Ingold, K. U. *J. Am. Chem. Soc.* **1976**, *98*, 1224.
(17) Wilkins, R. G. "The Study of Kinetics and Mechanism of Reactions of Transition Metal Complexes"; Allyn and Bacon: Boston, 1974; p 158.
(18) Walker, F. A.; Carlin, R. L.; Rieger, P. H. *J. Chem. Phys.* **1966**, *45*, 4181.
(19) Jordan, R. B.; Angerman, N. S. *J. Chem. Phys.* **1968**, *48*, 3983.
(20) Corden, B. J.; Rieger, P. H. *Inorg. Chem.* **1971**, *10*, 263.
(21) Farmer, J. B.; Herring, F. G.; Trapping, R. L. *Can. J. Chem.* **1972**, *50*, 2079.
(22) Carlton, L.; Lindsell, W. E.; Preston, P. N. *J. Chem. Soc., Dalton Trans.* **1982**, 1483.
(23) Lindsell, W. E.; Preston, P. N. *J. Chem. Soc., Dalton Trans.* **1979**, 1105.
(24) Brooks, H. B.; Sicilio, F. *Inorg. Chem.* **1971**, *10*, 2530.
(25) (a) Sicilio, F.; Florin, R. E.; Wall, L. A. *J. Phys. Chem.* **1966**, *70*, 47. (b) Brooks, H. B.; Sicilio, F. *Ibid.* **1975**, *79*, 2544.
(26) Goodman, B. A.; Raynor, J. B. *Adv. Inorg. Chem. Radiochem.* **1970**, *13*, 135.
(27) Gould, D. C.; Mason, H. S. *Biochemistry* **1967**, *6*, 801.
(28) McBryde, W. A. E. *Talanta* **1974**, *21*, 979.
(29) (a) Hänisch, G.; Kaden, Th. A.; Zuberbühler, A. D. *Talanta* **1979**, *26*, 563. (b) Zuberbühler, A. D.; Kaden Th. A. *Ibid.* **1979**, *26*, 1111.
(30) Maeder, M.; Gampp, H. *Anal. Chim. Acta* **1980**, *122*, 303.
(31) Gampp, H.; Maeder, M.; Zuberbühler, A. D. *Talanta* **1980**, *27*, 1037.
(32) Gampp, H. *Inorg. Chem.* **1984**, *23*, 1553.

gave the corresponding amide ligand, 4,7,10-triazatridecanediamide trihydrochloride (AMIDE·3HCl).[33b]

Measurement. A 2-mL portion of 1 M NaOH, 1 mL of 0.5 M KCl, and 1 mL of a solution that was 0.0395 M in Cu^{2+} and 0.0405 M in ligand (NIT) were mixed. A melting point tube was filled with this solution, sealed, and fixed within the cavity of an EPR spectrometer (Varian E 3, using 100-kHz field modulation, equipped with a 9.5-GHz microwave bridge).

A total of 24 EPR spectra were measured between 2800 and 3300 G at 295 K over a period of 350 min and recorded on chart paper. Instrument settings were as follows: 4-mW microwave power; 1.0-G modulation amplitude; 1-s time constant; 2 G s^{-1} scan rate; 6.2×10^5 receiver gain. The stable pentaphenylallyl radical[34] ($g = 2.0026$) was used as a standard and gave a signal at 3290 G at a microwave frequency of 9.417 GHz. A similar experiment was done with ligand AMIDE.[35]

Visible spectra were obtained with a Cary 118 C spectrophotometer from 5 mM solutions.

Data Reduction. The first-derivative EPR spectra (Cu(II)–NIT system) were digitized on an Apple II desk computer equipped with a Graphix Tablet (progam EPRDIG[36]). Each of the 24 recorded spectra was resolved into 41 digital points at equidistant intervals of 10 G between 2900 and 3300 G. The data are expressed in arbitrary units (au) and range from 0 to 75 au. The EPR data and the times at which each spectrum was taken were stored on diskette.

The calculations were done on a Hewlett-Packard HP 9835 desk computer with 128K memory, equipped with a HP 72225A plotter and a Heathkit H14 printer. The data were transferred from the Apple II to the HP 9835 through a serial interface HP 98036A (program TRANSFER[36]) and were evaluated with the program EPRKIN[36] (written in Basic), which consists of three parts: (i) The first one is a modified version of EIGEN[30] and represents the measured first-derivative EPR spectra in their eigenvector basis. This leads to a significant reduction of the amount of data to be handled in the iterative refinement of the parameters without any loss of significant information. The eigenvector representation also gives us the number of complexes occurring during the reaction. (ii) The second part is a modified version of ELORMA.[31] The program fits a sum of exponentials to the data set simultaneously, i.e. calculates the best set of rate constants (leading to the minimal square sum). Only estimates for the rate constants are needed, while the molar EPR absorptivities (i.e., the dI/dH for every H) are eliminated from the iterative refinement. The EPR spectra of the complexes are obtained noniteratively from the final set of rate constants by linear regression at the end of the calculation. (iii) The third part consists of several subroutines and allows us to plot the species distribution as a function of time, the titration curves at different magnetic fields, and the EPR spectra of the individual complexes. In addition, the double integration of the calculated spectra can be done.

Mathematical Methods. The mathematical methods used for the numerical evaluation of the kinetic data have been described elsewhere.[30,31] Therefore, it will only be outlined how the problem of determining rate constants and EPR spectra of the complexes formed during the reaction is formulated in order to do the mathematical treatment.

Given a set of S first-derivative EPR spectra measured at H discrete magnetic field strengths, the whole data set can be written as a matrix $\mathbf{Y}$ (S = number of rows; H = number of columns) (eq 1).

$$\mathrm{Y} = \begin{bmatrix} (\mathrm{d}I/\mathrm{d}H_1)_1 & (\mathrm{d}I/\mathrm{d}H_2)_1 & \cdots & (\mathrm{d}I/\mathrm{d}H_H)_1 \\ (\mathrm{d}I/\mathrm{d}H_1)_2 & & & \cdot \\ \cdot & & & \cdot \\ \cdot & & & \cdot \\ (\mathrm{d}I/\mathrm{d}H_1)_S & \cdots & \cdots & (\mathrm{d}I/\mathrm{d}H_H)_S \end{bmatrix} \tag{1}$$

Obviously, each row of $\mathbf{Y}$ is a spectrum obtained at a certain time, and each column is a kinetic curve observed at one particular magnetic field strength. If each spectrum is recorded with constant scan rate and if the time difference between two subsequent readings equals d, the time t_{sh} at which an element Y_{sh} has been obtained is given by eq 2.

$$t_{sh} = t(H_h)_s = t(H_0)_s + (h-1)d = t_s{}^0 + (h-1)d \tag{2}$$

In the chemical example studied, $P = 3$ absorbing species occur and two first-order consecutive steps are necessary to describe the kinetics (vide infra). Provided that Beer's law is valid, each measured spectrum is a linear combination of the unknown spectra of the complexes present in solution and each kinetic curve can be represented by a calculated expression $\mathbf{f}_h$ (eq 3).

$$\mathrm{f_h} = \begin{bmatrix} 1 & e^{-k_1 t_{1h}} & e^{-k_2 t_{1h}} \\ \cdot & \cdot & \cdot \\ \cdot & \cdot & \cdot \\ \cdot & \cdot & \cdot \\ 1 & e^{-k_1 t_{Sh}} & e^{-k_2 t_{Sh}} \end{bmatrix} \cdot \begin{bmatrix} a_{h,0} \\ a_{h,1} \\ a_{h,2} \end{bmatrix} = \mathrm{C_h \cdot a_h} \tag{3}$$

Obviously, $\mathbf{C}_h$ is dependent on the magnetic field strength due to the finite recording time of the spectra. Substituting t_{sh} (eq 2) into eq 3 allows one to decompose the exponentials (eq 4).

$$\mathrm{f_h} = \begin{bmatrix} 1 & e^{-k_1(t_1{}^0+(h-1)d)} & e^{-k_2(t_1{}^0+(h-1)d)} \\ \cdot & \cdot & \cdot \\ \cdot & \cdot & \cdot \\ \cdot & \cdot & \cdot \\ 1 & e^{-k_1(t_S{}^0+(h-1)d)} & e^{-k_2(t_S{}^0+(h-1)d)} \end{bmatrix} \cdot \begin{bmatrix} a_{h,0} \\ a_{h,1} \\ a_{h,2} \end{bmatrix}$$

$$= \begin{bmatrix} 1 & e^{-k_1 t_1{}^0} & e^{-k_2 t_1{}^0} \\ \cdot & \cdot & \cdot \\ \cdot & \cdot & \cdot \\ \cdot & \cdot & \cdot \\ 1 & e^{-k_1 t_S{}^0} & e^{-k_2 t_S{}^0} \end{bmatrix} \cdot \begin{bmatrix} a_{h,0} \\ a_{h,1} e^{-k_1(h-1)d} \\ a_{h,2} e^{-k_2(h-1)d} \end{bmatrix} = \mathrm{C \cdot a_h}^* \tag{4}$$

Finally, the matrix of the experimental data $\mathbf{Y}$ (eq 1) can be represented by a calculated matrix $\mathbf{F}$ (eq 5).

$$\mathbf{F} = \mathbf{C \cdot A} \tag{5a}$$

$$\mathrm{A}^* = \begin{bmatrix} a_{1,0} & a_{2,0} & \cdots & a_{H,0} \\ a_{1,1} & a_{2,1} e^{-k_1 \mathrm{d}} & \cdots & a_{H,1} e^{-k_1(H-1)d} \\ a_{2,1} & a_{2,2} e^{-k_2 d} & \cdots & a_{H,2} e^{-k_2(H-1)d} \end{bmatrix} \tag{5b}$$

$\mathbf{A}^*$ can be written as a function of $\mathbf{C}$ (eq 6),[31,37] and $\mathbf{R}$, the matrix of the residuals, depends only on the nonlinear parameters k_1 and k_2 (eq 7). Consequently, only these two parameters have to be refined

$$\mathbf{A}^* = (\mathbf{C}^\mathrm{T}\mathbf{C})^{-1}\mathbf{C}^\mathrm{T}\mathbf{Y} \tag{6}$$

$$\mathbf{R} = \mathbf{Y} - \mathbf{F} = \mathbf{Y} - \mathbf{C}(\mathbf{C}^\mathrm{T}\mathbf{C})^{-1}\mathbf{C}^\mathrm{T}\mathbf{Y} \tag{7}$$

iteratively in the least-squares procedure. With use of the Newton–Gauss–Marquardt algorithm,[38] for a given set of estimated parameters, at each magnetic field strength H_h, the Jacobian $\mathbf{J}_h$ (i.e., the matrix containing the derivatives of $\mathbf{f}_h$ with respect to the parameters), $(\mathbf{J}_h{}^\mathrm{T}\mathbf{J}_h)^{-1}$, and $\mathbf{J}_h{}^\mathrm{T}\mathbf{r}_h$ have to be calculated and shifted parameters are obtained according to eq 8.[39]

$$\mathbf{p}_{\mathrm{It}+1} = \mathbf{p}_{\mathrm{It}} + (\mathbf{J}^\mathrm{T}\mathbf{J})^{-1}\mathbf{J}^\mathrm{T}\mathbf{R} \tag{8}$$

$$\mathbf{J}^\mathrm{T}\mathbf{J} = \sum_{h=1}^{H} \mathbf{J}_h{}^\mathrm{T}\mathbf{J}_h \qquad \mathbf{J}^\mathrm{T}\mathbf{R} = \sum_{h=1}^{H} \mathbf{J}_h{}^\mathrm{T}\mathbf{r}_h$$

The parameters can be determined either from eq 3 or from eq 5, the only difference being that in the first case $\mathbf{C}_h$ has to be calculated

---

(33) (a) Maeder, M. Ph.D. Thesis, University of Basel, 1980. (b) Gampp, H.; Haspra, D.; Maeder, M.; Zuberbühler, A. D. *Inorg. Chem.*, in press.

(34) Solar, S. L. *J. Org. Chem.* **1963**, *28*, 2911.

(35) The measured spectra for the Cu(II)–AMIDE system indicated only an extremely slow reaction. No significant changes were observed over several hours, and no attempt was made to evaluate the data.

(36) Listings of the programs are available upon request.

(37) (a) Richards, F. S. G. *J. R. Statist. Soc., Ser. B* **1961**, *23*, 469. (b) Lawton, W. H.; Sylvestre, E. A. *Technometrics* **1971**, *13*, 461.

(38) Marquardt, D. W. *J. Soc. Ind. Appl. Math.* **1963**, *11*, 431.

(39) The Newton–Gauss–Marquardt algorithm has been described in detail for cases where both linear and nonlinear parameters occur.[31]

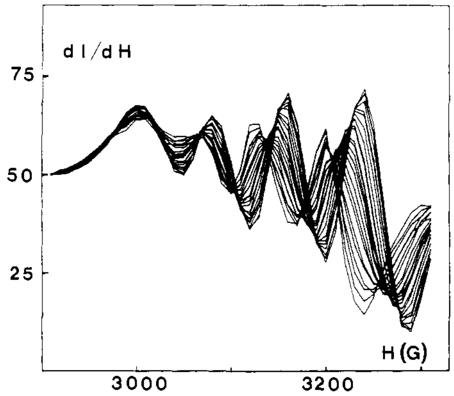

Figure 1. Plot of the kinetic EPR data for the hydrolysis of the cupric complex of 4,7,10-triazatridecanedinitrile (NIT) in 0.5 M aqueous NaOH (25 °C; $[Cu^{2+}]_{tot} = 0.01975$ M; $[NIT]_{tot} = 0.02025$ M).

separately for each magnetic field strength, while in the second case only one such matrix has to be computed for each iteration.

Using eq 5 opens a way to do the complete numerical treatment in much shorter time and with a minimum of computer space. For a system of P absorbing species, the data matrix **Y** (eq 1) can be formulated as a linear combination of P eigenvectors.[30] In our example with $P = 3$, **Y** can be represented by $\mathbf{Y}_{ev}$ (eq 9), i.e. as a product of

$$Y_{ev} = \begin{bmatrix} L_{11} & L_{12} & L_{13} \\ \cdot & \cdot & \cdot \\ \cdot & \cdot & \cdot \\ \cdot & \cdot & \cdot \\ L_{S1} & L_{S2} & L_{S3} \end{bmatrix} \cdot \begin{bmatrix} E_{11} & \cdots\cdots & E_{1H} \\ E_{21} & \cdots\cdots & E_{2H} \\ E_{31} & \cdots\cdots & E_{3H} \end{bmatrix} \qquad (9)$$

$$= \mathrm{L} \cdot \mathrm{E}$$

two matrices **L** and **E**. **E** (dimension $3 \times H$) contains the eigenvectors and **L** (dimension $S \times 3$) the respective linear coefficients.[40] The eigenvector representation thus yields the number of absorbing species and leads to a short-hand notation of the experimental data. Further benefit comes from the fact that **L** can be used instead of **Y** in the least-squares procedure.[30,41] Hence, irrespective of the number of magnetic field strengths at which the spectra have been recorded, the iterative refinement of the parameters can be done as if the kinetic experiment had been carried out at $P = 3$ magnetic fields only. In our case, instead of handling $S \times H = 24 \times 41 = 984$ data points, we have to deal with $S \times 3 = 72$ data only, which saves both computer time and memory. It should be emphasized that the use of **L** in the parameter refinement is only possible due to the fact that **F** can be written according to eq 5, i.e. that the finite recording time of the spectra can be ignored.

After the nonlinear parameters are obtained, the spectra of the species occurring in the kinetic system are calculated from eq 6.

Results and Discussion

Eigenvector Analysis. The measured data written according to eq 1 were represented in their eigenvector basis (eq 9). Matrix rank analysis showed that the data could be represented by three eigenvectors. The overall standard deviation between the experimental data and their eigenvector representation is 0.4 au (corresponding to less than 1% of the average measured first-derivative intensity) and thus equals the error introduced by digitizing the spectra. This can also be taken as a quantitative measure for the data quality. Because the sample was in a fixed position throughout the experiment, errors due to repositioning or due to different EPR tubes were avoided (Figure 1).

Rate Constants for the Hydrolysis of the Copper(II)-NIT Complex. Whereas the eigenvector analysis is completely independent of the choice of a chemical model, rate constants can only be obtained on the basis of a particular reaction scheme. For the studied reaction, matrix rank analysis indicated three absorbing species and therefore a two-step mechanism (I) can be expected. Assuming two first-order

$$\mathbf{1} \xrightarrow{k_{12}} \mathbf{2} \xrightarrow{k_{23}} \mathbf{3} \qquad (I)$$

consecutive reactions, the calculated rate constants $k_{12} = (3.55 \pm 0.07) \times 10^{-4}\ s^{-1}$ and $k_{23} = (8.5 \pm 0.3) \times 10^{-5}\ s^{-1}$ (corresponding to half-lives of 32 and 136 min) yield the species distribution shown in Figure 2. The overall standard deviation between the experimental data **Y** and their calculated analogues **F** (eq 1 and 5) is 0.5 au. This value is only slightly larger than the one obtained from the eigenvector representation and the chosen reaction scheme (I) thus leads to a satisfying mathematical description of the data. Figure 3 shows the good fit of the experimental points by calculated curves, indicating that no systematic deviations occur.

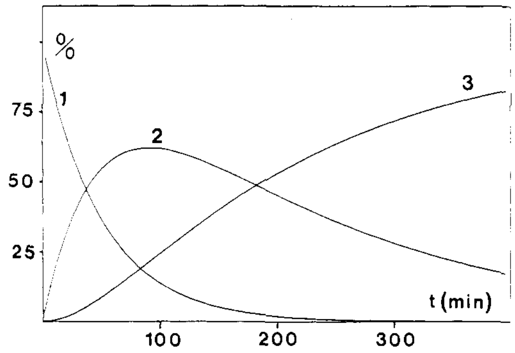

Figure 2. Species distribution as a function of time for the Cu(II)-NIT complexes using calculated rate constants.

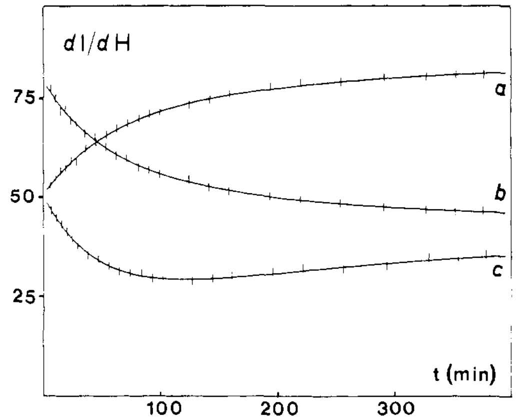

Figure 3. Kinetic curves for the Cu(II)-NIT system: (a) 3150 G; (b) 3110 G; (c) 3260 G. Experimental data: bars of length 4σ. Calculated curve: —.

From Figure 1 it is evident that the measured spectra are strongly overlapping and that there is no way to determine the concentrations of the different species by simply integrating. Moreover, the rate constants were calculated from all the information contained in the data set. No care had to be taken in order to select "relevant" magnetic field strengths, which would require some information about the chemical system prior to the calculation.

EPR Spectra of the Copper(II)-NIT Complexes. The calculated spectra show four lines each (Figure 4), consistent with the interaction of an unpaired electron with a copper nucleus of nuclear spin $\mathbf{I} = {}^3/_2$.[26] No additional hyperfine structure due to the interaction with the ^{14}N nuclei ($I = 1$) is seen. Each spectrum has an asymmetrical shape; the heights of the peaks increase with the magnetic field. This means that at room temperature the complexes do not rotate fast enough

---

(40) The mathematical basis and a program to do the eigenvector representation are described.[30]

(41) Sylvestre, E. A.; Lawton, W. H.; Maggio, M. S. *Technometrics* **1974**, *16*, 353.

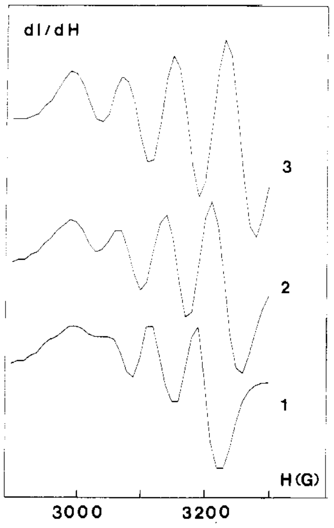

Figure 4. Calculated EPR spectra of the Cu(II)–NIT complexes (cf. reaction scheme I).

Table I. Spectral Parameters of Cu(II)-NIT and Related Complexes

species	g_{av}[a,b]	A_{av}, mK	I,[c] au	λ_{max}, nm
1	2.125	6.64	562	680
2	2.111	7.19	554	580
3	2.103	7.76	529	580
$CuNITH_{-1}$[d]	2.113	6.24		603[e]
CuAMID[f]	2.102	7.85		580

[a] The values for g_{av} and A_{av} were determined graphically. [b] The magnetic field was calibrated by using the signal of pentaphenylallyl[34] as standard. [c] Double integral calculated between 2900 and 3300 G by numerical integration. [d] pH 11.5. [e] From ref 33b. [f] In 0.5 M NaOH (cf. ref 35).

that the anisotropic terms in the Hamiltonian are averaged to zero, which would result in a symmetric spectrum. A similar anisotropy has been found for the room-temperature EPR spectra of copper(II) dipeptide[27] and diamide[32] complexes.

In the spectrum of **1**, the two low-field lines are not well separated. This is not an artifact produced by the mathematical treatment, as the same feature is evident in the initially recorded spectra.

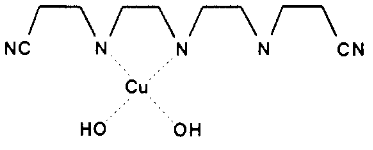

1

The reliability of the calculation can be further tested by determining the spin concentration for each complex. This is done by double integrating the calculated first-derivative spectra with respect to the magnetic field strength. As there is one unpaired electron in each complex, the integration should give the same result for the three spectra. The calculated integrals indeed differ by less than 5% (Table I). It should be emphasized that this result, which is required by the theory, has not been introduced into the algorithm used. Moreover, no information at all with regard to the shape of the spectra was used in the mathematical procedure.

The values for g_{av} decrease from **1** over **2** to **3**, while those for A_{av} show the reversed order (Table I). As has been shown for a great number of square-planar cupric complexes, the values for g and A depend on the equatorial donor atoms and on the charge of the complexes.[42,43] Increasing donor strength and increasing negative charge both result in an increase of the cubic ligand field and produce smaller values for g, greater values for A, and a shift of the d–d band to shorter wavelengths.[44]

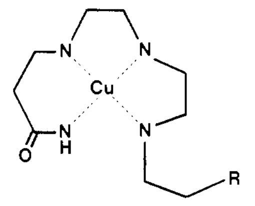

2 R=CN
3 R=CONH$_2$

Structure of the Copper(II)–NIT Complexes. The spectrum of the initially formed species **1** is different from that observed for $CuNITH_{-1}^+$ (Table I). Both EPR and visible spectra suggest that **1** has a weaker ligand field; i.e., most likely only two amino groups are coordinated equatorially, whereas the remaining positions are occupied by two OH^-. As for $CuNITH_{-1}^+$ no significant apical coordination is evident,[33b] and the same can be assumed for **1**.

The increased ligand field for **2** and **3** is explained by a hydrolysis of the nitrile groups leading to strongly coordinating amide sites. Nitriles are rather inert in basic solution, but upon coordination to metal ions the rate of hydrolysis is enhanced by several orders of magnitude. This is known both for kinetically inert (e.g., Co(III)[45]) and for the labile (e.g., Co(II)[46] and Cu(II)[47]) systems. The influence of proximity effects has been shown recently by using a tetraaza macrocyclic cupric complex with a nitrile function in a side chain.[48] The amide group too undergoes a metal-promoted hydrolysis, but only if the amide oxygen is coordinating.[44] In cases where stable chelate complexes can be formed, the amide is deprotonated, coordinates via nitrogen,[49] and is thus protected from further hydrolysis.[44,48]

For the first step of the Cu(II)–NIT hydrolysis we can expect the formation of one amide group, most likely by an intramolecular attack of OH^- to a coordinated nitrile.[48] The resulting complex **2** is equatorially coordinated by a deprotonted amide and by three amino nitrogens. For the second nitrile group, only a weak apical interaction can occur and because no internal attack of OH^- is possible as in **1** this reaction proceeds at slower rate.

The structure of **3** was confirmed in an independent experiment, where instead of the nitrile ligand (NIT) the corresponding diamide (AMIDE) was used.[35] Both EPR and visible spectra[50] were identical with those of **3**, and thus the final product of the hydrolysis is the Cu(II)–AMIDE complex. In structures **2** and **3** only the equatorial coordination is shown. If no other interaction would occur, the spectra of **2** and **3** should be almost identical. However, EPR spectra contrary to the visible absorptions show a marked difference. As EPR parameters are rather sensitive to distortion,[43] an additional

---

(42) Peisach, J.; Blumberg, W. E. *Arch. Biochem. Biophys.* **1974**, *165*, 691.

(43) Addison, A. W. "Copper Coordination Chemistry: Biochemical and Inorganic Perspectives"; Karlin, K. D., Zubieta, J., Eds.; Adenine Press: New York, 1983; p 109.

(44) Sigel, H.; Martin, R. B. *Chem. Rev.* **1982**, *82*, 385.

(45) Buckingham, D. A.; Keene, F. R.; Sargeson, A. M. *J. Am. Chem. Soc.* **1973**, *95*, 5649.

(46) Clark, C. R.; Hay, R. W. *J. Chem. Soc., Dalton Trans.* **1974**, 2148.

(47) Breslow, R.; Fairweather, R.; Keana, J. *J. Am. Chem. Soc.* **1967**, *89*, 2135.

(48) Schibler, W.; Kaden, Th. A. *J. Chem. Soc., Chem. Commun.* **1981**, 603.

(49) Kaden, Th. A.; Zuberbühler, A. D. *Helv. Chim. Acta* **1974**, *57*, 286.

(50) In a reaction that takes several days, the absorption maximum is shifted from 580 to 630 nm, where the cupric complex of the corresponding dicarboxylate ligand has its maximum.[33b] This is found both with NIT and with AMIDE and means that the coordinated amide too is hydrolyzed although at very slow rate.

apical coordination of the fifth donor group must be assumed for **3**.

Conclusions

The present study shows that rate constants and spectra of complexes can be obtained from EPR solution spectra.

The use of appropriate mathematical methods allows one to do the numerical evaluation in a straightforward manner even on a desk computer. Only initial estimates for the rate constants are necessary, while no information with regard to the spectra of the complexes is needed. No care has to be taken to select the data such that only distinct complexes give rise to a signal, since by doing the calculation on the complete data set simultaneously, all the information from the measurement is used.

Eigenvector representation not only yields the number of absorbing species but allows one to do the numerical treatment using minimal computer time and memory.

The spectra of the different chemical species are easily obtained, and valuable structural information can be derived from this. While this is also true for spectrophotometry, the EPR method has the advantage that the spin concentrations can be calculated for each complex, which helps to confirm the results of the mathematical analysis.

The results of this study show that EPR spectroscopy indeed is a useful method for the elucidation of reaction mechanisms. Because the mathematical evaluation of the data is straightforward, EPR measurements should be included in kinetic studies whenever possible.

Acknowledgment. Dr. M. Maeder provided the ligand, and Prof. F. Gerson allowed to use his EPR spectrometer (both from the University of Basel). This work was supported by the Swiss National Science Foundation (Grant No. 2.213-0.81).

Registry No. **1**, 91994-70-6; **2**, 91994-71-7; **3**, 91994-72-8.

Contribution from the Department of Chemistry,
University of New Brunswick, Fredericton, New Brunswick, Canada E3B 6E2

Effect of Anions on Redox Reactions. 1. Chromium(II) Reduction of Bis(pentane-2,4-dionato)(ethylenediamine)cobalt(III) in the Presence of Chloride Ions

NITA A. LEWIS* and ANANDA M. RAY

Received October 25, 1983

The effect of chloride ions on the Cr(II) reduction of $[Co(en)(ptdn)_2]^+$ was studied. The rate for the outer-sphere pathway was twice that of the uncatalyzed reaction ($k(25.0\ ^\circ C) = (4.86 \pm 0.04) \times 10^{-3}\ M^{-1}\ s^{-1}$, $\Delta H^* = 17 \pm 1$ kcal mol^{-1}, $\Delta S^* = -13 \pm 3$ eu) whereas the rates for the inner-sphere pathways were practically unaffected. The kinetic parameters for the monobridged pathway were $k(25.0\ ^\circ C) = (2.97 \pm 0.02) \times 10^{-3}\ M^{-1}\ s^{-1}$, and those of the dibridged path were $k(25.0\ ^\circ C) = (1.46 \pm 0.02) \times 10^{-3}\ M^{-1}\ s^{-1}$, $\Delta H^* = 13 \pm 1$ kcal mol^{-1}, and $\Delta S^* = -27 \pm 1$ eu. No chloride could be detected in the inner-sphere electron-transfer products.

Introduction

It has been recognized for a very long time[1] that redox reactions between like-charged ions in solution may be markedly accelerated by the presence of ions of the opposite charge. It is generally assumed that the ion catalyst operates by coordinating to one of the reactants, thereby lowering the charge on this complex and reducing the Coulombic repulsion between the reacting species. The purpose of the present investigation was to see if there are substantial differences between the way the ion catalyst affects an outer-sphere as opposed to an inner-sphere process. The ultimate aim of this approach was to try to find a method involving ion catalysis that would allow one to distinguish between these two possible mechanisms of electron transfer, especially in cases in which the product criterion fails.[2]

The model reaction we have used to investigate this effect is the Cr(II) reduction of $[Co(en)(ptdn)_2]^+$ (where ptdn is the abbreviation used for pentane-2,4-dionato, also called acetylacetonato or acac) in the presence of chloride ions. This reaction was selected because, at least in perchlorate media,[3,4] the reduction proceeded simultaneously by all three possible mechanisms—outer sphere, monobridged inner sphere, and dibridged inner sphere.

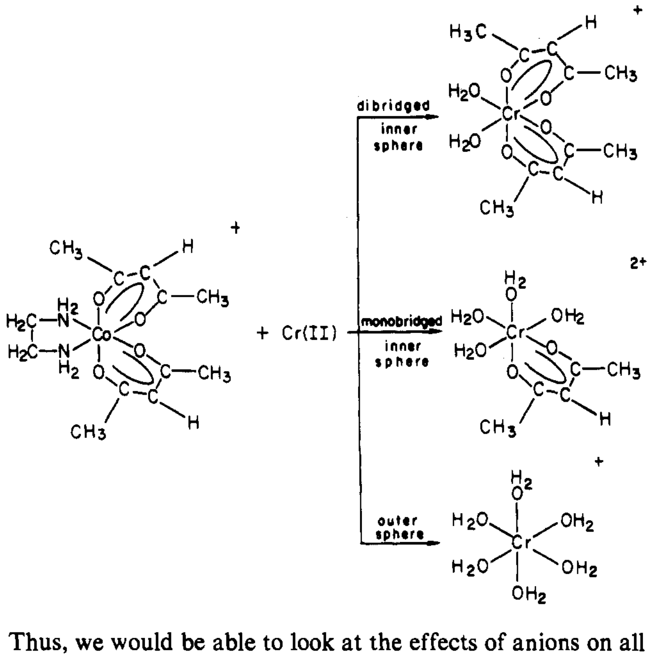

Thus, we would be able to look at the effects of anions on all three mechanisms for identical reactants under identical

---

[1] Taube, H.; Myers, H. *J. Am. Chem. Soc.* **1954**, *76*, 2103.

[2] McAuley, A. *Inorg. React. Mech.* **1976**, *4*, 9.

[3] Balahura, R. J.; Lewis, N. A. *J. Chem. Soc., Chem. Commun.* **1976**, 268.

[4] Balahura, R. J.; Lewis, N. A. *J. Am. Chem. Soc.* **1977**, *99*, 4716.